J Electr Eng Technol Vol. 8, No. 2: 376-384, 2013
http://dx.doi.org/10.5370/JEET.2013.8.2.376

ISSN(Print) 1975-0102
ISSN(Online) 2093-7423

Real-Time Heart Rate Monitoring System based on Ring-Type Pulse Oximeter Sensor

Seung-Min Park*, Jun-Yeup Kim*, Kwang-Eun Ko*, In-Hun Jang and Kwee-Bo Sim†**

Abstract – With the continuous aging of the populations in developed countries, the medical requirements of the aged are expected to increase. In this paper, a ring-type pulse oximeter finger sensor and a 24-hour ambulatory heart rate monitoring system for the aged are presented. We also demonstrate the feasibility of extracting accurate heart rate variability measurements from photoelectric plethysmography signals gathered using a ring-type pulse oximeter sensor attached to the finger. We designed the heart rate sensor using a CPU with built-in ZigBee stack for simplicity and low power consumption. We also analyzed the various distorted signals caused by motion artifacts using a FFT, and designed an algorithm using a least squares estimator to calibrate the signals for better accuracy.

Keywords: Heart rate sensor, Photoelectric plethysmography, Heart rate variability, Blood volume pulse, Biomedical monitoring, U-health care.

1. Introduction

A major issue of an aging society with fewer children is the need of the elderly and the handicapped for better living conditions. To address this issue, many social welfare services, and supporting machines or systems for them, have been developed [1-3]. In particular, the responsibility of providing healthcare for the elderly and handicapped is now being shared by the families and various organizations. The elderly often find it difficult to cope with medical emergencies. The best solution to this problem may be to provide ubiquitous health care which allows out-of-hospital monitoring.

In the past decade, a considerable amount of research has been dedicated to ubiquitous computing in health care. Exhibition projects such as "u-chronic care" have become highly complex. The u-chronic care provides chronic sufferers of disease, particularly the elderly, with telemedicine services, including blood sugar and heart monitoring, through a university hospital data collection center. The demand for this type of service is expected to increase in the future. For the success of a u-health care service, two conditions are essential. First, signals must be clearly measured without the awareness of the carrier, and second, the acquired data must be transferred wirelessly. Currently, u-chronic care is available for the collection of biomedical signals such as electrocardiogram (ECG), heart rate (HR), blood pressure, and blood sugar rate. Among these, heart rate signal data, which possesses essential health information that pertains to life-threatening problems, can be acquired most easily. Previous commercial ambulatory heart rate monitoring devices were incorporated into watches and used by athletes for weight management and general fitness. However, it is uncomfortable to wear such devices for long durations because the transmitter and strap must be worn around the chest. For example, Yang proposed a ring-type heart rate sensor and developed some prototypes [4, 5]. The prototypes were elementary in form, and to our knowledge they have not been commercially produced. In contrast, we designed and developed a commercially-viable ring-type sensor that can be used for 24-hour ambulatory heart rate monitoring. Practical application of efficient, low-cost wireless communication technologies such as Bluetooth, ZigBee, and RFID can be extended to the design and use of medical monitoring equipment. Consequently, these technologies have become the most pursued applications in the field of sensor networks, particularly in relation to the development of medical services to cope with emergent health crises in seniors who live independently. In our project, we have also constructed a sensor network system for remotely monitoring individuals and assisting them in seeking help from other people in emergency situations.

In the next section, we describe the methodology for acquiring a photoelectric plethysmography signal from a finger, and show the hardware specifications of the ring sensor. We also present our sensing program, RF-based communication, and power requirements of the ring sensor. Section III presents the monitoring system, signal processing algorithms for the estimation of HR, and a discussion of the resolution of the sensing data. Experimental results and

† Corresponding author: School of Electrical and Electronics Engineering, Chung-Ang University, Seoul, Korea (kbsim@cau.ac.kr)
* School of Electrical and Electronics Engineering, Chung-Ang University, Seoul, Korea ({sminpark, jy915, kkeun}@cau.ac.kr)
** Korea Institute of Industrial Technology, Korea (inhuns@kitech.re.kr)
Received: September 20, 2011; Accepted: November. 1, 2012

discussion are presented in Section IV, followed by our conclusion and proposed future work in Section V.

2. Methodology

2.1 Measurements of heart rate signals

A finger photo-plethysmograph (PPG) is a noninvasive transducer that measures relative changes in blood volume or the oxygen saturation in a subject's finger. The blood volume pulse (BVP) sensor reads the relative changes in blood volume. The pulse oximeter reads the oxygen saturation in the arterial blood. These instruments employ the same measuring principle, which is based on the red and infrared light absorption characteristics of oxygenated and deoxygenated hemoglobin. Oxygenated hemoglobin absorbs more infrared light and allows more red light to pass through. Deoxygenated (or reduced) hemoglobin absorbs more red light and allows more infrared light to pass through. Fig. 1 shows the absorption spectra of Hb and HbO2 [6].

With each heartbeat, the change in arterial blood volume momentarily increases or decreases the amount of Hb and HbO2. This results in the absorption of more light during the systolic phase and less light during the diastolic (resting) phase of the heart during any given beat. The photodiode output level is affected by variation in the level of light absorption. Hence, we obtain a waveform output level and determine the peaks between heartbeats. We can estimate the heart rate (number of beats per minute) from the measured peaks. The pulse oximeter determines the oxygen saturation from the photodiode output values using the following equation:

$$SaO_2 = \frac{[HbO_2]}{[Total\ \ Haemoglobin]}(\%) \quad (1)$$

where, $[Total\ Haemoglobin]=[HbO_2]+[Hb]$.

Two methods are employed for detecting light passing through the finger: the transmission method and the reflectance method. In the transmission method, as shown in Fig. 2 (a), the emitter and photodetector are placed opposite each other with the finger in between. Light can then pass through the finger. In the reflectance method, as shown in Fig. 2 (b), the emitter and photodetector are placed beside each other and on top of the measuring site. The transmission method is the more commonly used method; however, in this paper, reflectance method is considered to reduce its size.

2.2 System configuration of the ring sensor

Our proposed ring-sensor, acquires PPG data, processes it, and then transmits it to a telemetry manager (e.g. cell phone) which communicates it wirelessly and monitors the heart rate of the user. Therefore the ring sensor functionally can be divided into four blocks: the sensor block, processing block, RF block and power block, as shown in Fig. 3.

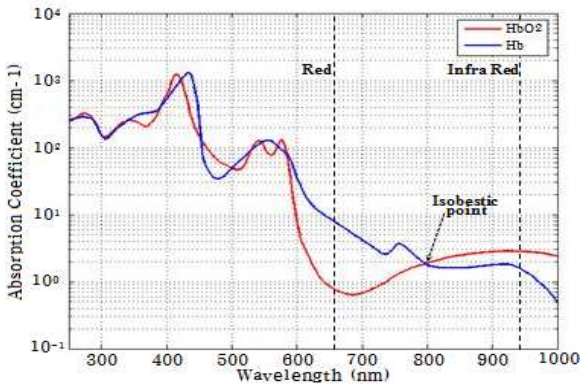

Fig. 1. Absorption spectra of Hb and HbO2 [6]

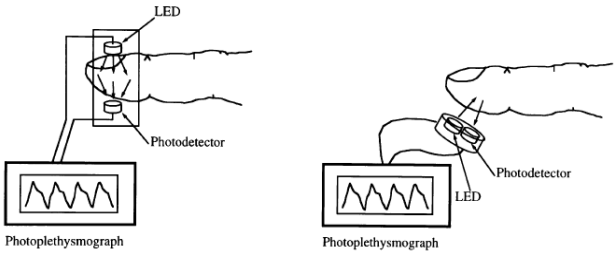

(a) (b)

Fig. 2. Type of PPG sensor [7]

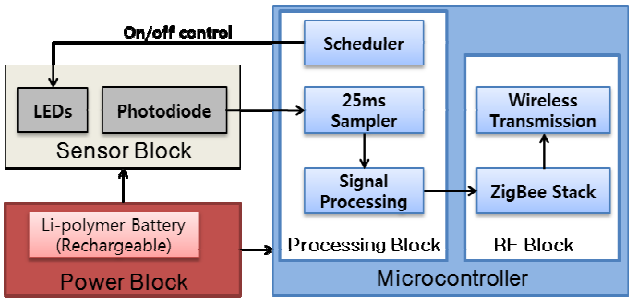

(a) Block diagram of the ring sensor

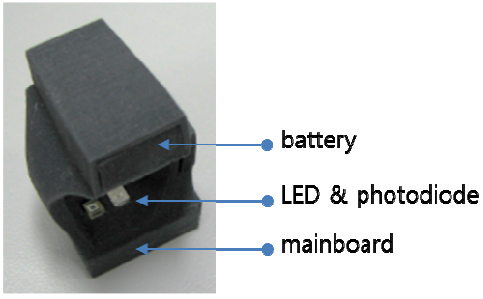

(b) Reflectance type of ring-sensor prototype

Fig. 3. System configuration of the ring sensor

The sensor block consists of a red LED, an infrared LED, and a photodiode (which is the light-to-frequency converter [8]). All parts can be switched on or off by a micro-controller unit (MCU) which provides proper brightness with minimum current consumption. The output of the sensor block is a square wave with frequency directly proportional to the light intensity.

The MCU is an MG2455-F48 chip which integrates 8-bit microcontroller for processing block and RF module for consisting RF block into a single die [9].

2.3 Control scheme for data acquisition

The MCU program has three main parts: a 25ms sampler with a scheduler for controlling the sensor block; a basic signal processing component; and an RF communication component.

The 25ms scheduler switches the LED and photodiode as shown in Fig. 4. When the LED and photodiode are turned on, the output of photodiode is a square wave with frequency directly proportional to the light intensity.

The basic signal processing component converts the interrupted signals triggered by square-wave-type photodiode outputs into time interval values of the corresponding square wave every 25ms. The intervals of the first two square waves can be acquired and then used as the sample values for calculating the heart rate. After one data is acquired, the LED and photodiode are turned off by the 25ms scheduler until the next sampling period in order to reduce power consumption. A total of 256 data is obtained to calculate heart rate.

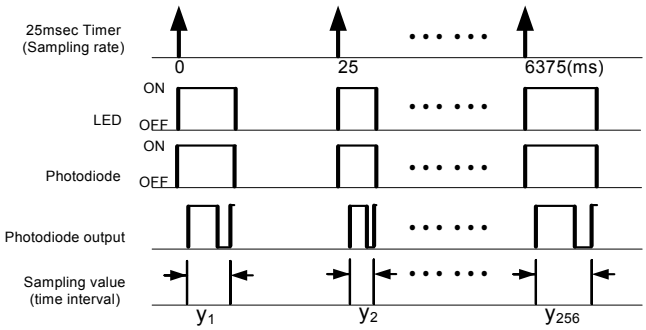

Fig. 4. Control scheme for data acquisition

2.4 Selection of the zigbee standard

Wireless personal area networks (WPANs) such as IrDA, Bluetooth, ZigBee, and UWB, have been developed for their own markets. In this study, we constructed a ZigBee network with a stand-alone coordinator and end devices. The base station, a PC, functions as our stand-alone coordinator and the ring-type heart rate sensors are our end devices. The favorable characteristics of our ring sensor, which are listed as follows, were the reasons for selecting the ZigBee standard:

- The data transmitted between the ring sensor and the monitoring system is not overwhelming to the system.
- The transmission distance is relatively long.
- The power consumption is low.
- The extension to the sensor network is prominent.

The ring sensor collects 256 samples of data and performs fast Fourier transform (FFT) to calculate the heart rate. Because each data sample contains 2 bytes, the sensing data which must be transmitted comprises 512 bytes. The ZigBee standard limits the payload of a single transmission to 64 bytes. Therefore, the ring sensor should transmit the sensing data eight times.

2.5 Control of power consumption

Since the ring-type sensor uses batteries, we require small batteries to fit the ring size. As the capacity of a battery is proportional to its size, the limited battery capacity of the ring sensor demands that it have very low power consumption. Therefore, we performed the on/off control of the LED, the photodiode, and the RF block to minimize power consumption. Fig. 5 shows a timing diagram indicating the control of the aforementioned parameters for the type 2 25ms sampler.

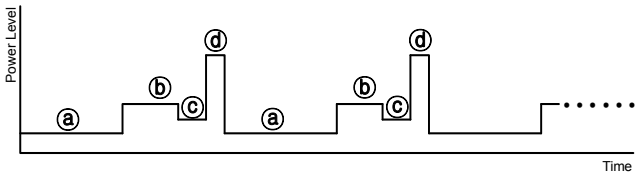

Fig. 5. Timing diagram to control the ring sensor

The durations corresponds to the following states:

- The duration ⓐ is a sleeping state.
  : MCU enters power down mode/ RF block is off.
- The duration ⓑ is a sensing state.
  : MCU wakes up, LED and photodiode is on.
- The duration ⓒ is a signal processing state.
  : LED and photodiode is off, RF block is off.
- The duration ⓓ is a transmitting state.
  : LED and photodiode is off, RF block is on.

The battery life of our ring sensor can be estimated by using the following equation:

$$lifetime(day) = \frac{battery\,capacity(mA) \times 3600(\sec) \times 1000(ms)}{power@active_{day} \times power@sleep_{day}} \quad (2)$$

where, $power@active_{day}$ = ($power@sensing \times duration\_sensing_{period}$ + $power@processing \times duration\_processing_{period}$ + $power@Tx \times duration\_Tx_{period}$) × $num\_sensing_{day}$

$$power@active_{day} = (power@sensing \times ⓑ + power@processing \times ⓒ + power@Tx \times ⓓ) \times num\_sensing_{day} \quad (3)$$

$$power@sleep_{day} = (3600(\sec) \times 24(hour) \times 1000(ms) - active\ time@day) \times power@sleep \quad (4)$$

$$active\ time@day = (duration\_sensing_{period} + duration\_processing_{period} + duration\_Tx_{period}) \times num\_sensing_{day} \quad (5)$$

where, ⓑ= $duration\_sensing_{period}$, ⓒ= $duration\_processing_{period}$, and ⓓ= $duration\_Tx_{period}$

We must transmit 512bytes during the sensing period; however, we cannot determine the payload over 64bytes to follow the ZigBee standard. Moreover, because the MG2455 does not have sufficient memory space, we must send the data as soon as the ring sensor collects 64bytes. In this case, approximately 2ms are required to transmit approximately 64-byte payloads at 250Kbps. The RF-block must be powered on for approximately 16ms so that all the sensing data are transmitted. The MG2455 consumes approximately 31 mA in transmit mode and approximately 26 mA in receiving mode. In our project, when we used a battery with a capacity of 80mA/h, 25ms sampler which acquired a biomedical signal every 4 min, the estimated lifetime was approximately 6.1 days.

3. Monitoring System

3.1 Structure of the Monitoring System

Our monitoring system contains three principal devices: a ring sensor, a telemetry manager, and a monitoring station server. The ring sensor, which is worn around the user's finger, collects the heart rate data and sends it to the telemetry manager connected wirelessly by short range. The telemetry manager stores and processes that data, estimates the heart rate, and determines whether or not the person is in an emergency state. When an emergency develops, the telemetry manager quickly and automatically sends short messaging services (SMS) and instant messages via the WCDMA or the internet (TCP/IP) to the monitoring station server. The telemetry manager may be a mobile phone or an internet phone. We developed the mobile phone application using the ZigBee USIM card, made jointly by Radiopulse and SK Telecom. The Zigbee USIM card integrates a Zigbee single chip and USIM, for 3G mobile phone, turning the device into a gateway between the Zigbee network and the cellular/IP network to collect and display information. Then, the monitoring station server asks for a rescue party or asks for a help to career. Fig. 6 shows the general procedures by which emergency messages are transferred to the career or rescue team.

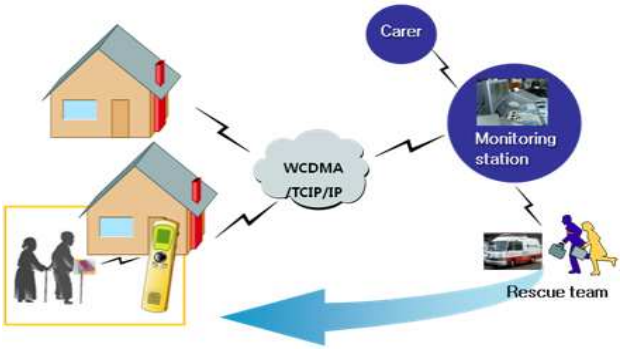

Fig. 6. Structure of the monitoring system

3.2 Overview of the monitor program

We now describe how the algorithms calculate the heart rate from raw biomedical data remotely received from the ring sensor. Two types of algorithms are used: a software peak detector, and FFT analysis.

1) Selection of sampling rate and sampling time:

In order to design a heart rate sensor, we must first determine a range for the heart measurement, and then we need to obtain samples at a fixed rate. The range of heart rate was chosen from 20 to 200bpm, which is appropriate for detecting emerging health crises. For 20bpm, or 0.3bps, that needs at least 6.6sec which is 2-periods corresponding for minimum number of periods for catching one period. Generally, FFT analysis is one of the most efficient methods for analyzing the frequency about a periodic signal. We selected a sampling rate of 256bytes FFT by using the following equation.

$$\text{Sampling rate} = \frac{6600}{256} \fallingdotseq 25[\text{ms}] \quad (6)$$

For 200bpm, or 3.3Hz, the minimum sampling rate would be approximately 7 Hz based on the Nyquist theorem. A 25ms sampling rate, or 40Hz, is also satisfied with this condition. In this case, the total sampling time for collecting 256 measurements was 6400ms.

2) Software peak detector:

The monitor program shown in Fig. 7 calculates the HR using an algorithm based on a software peak detector; this program is designed to mimic the hardware peak detector designed by Jeff Bachiochi [10, 11]. However, this peak detector misses the maximum or minimum peak when there is a shift downward or upward because of a change in the dc level, or a change in the absorption constant. To prevent such cases, Bachiochi used a leakage adjustment. However, in actual applications, there is a limit to the use of the leakage adjustment in the ambulatory ring sensor. The biomedical signal is very weak and is easily distorted

by the user's movement or by environmental perturbation. In addition, this algorithm has another drawback: the resolution becomes unacceptable with an increase in the count of beats.

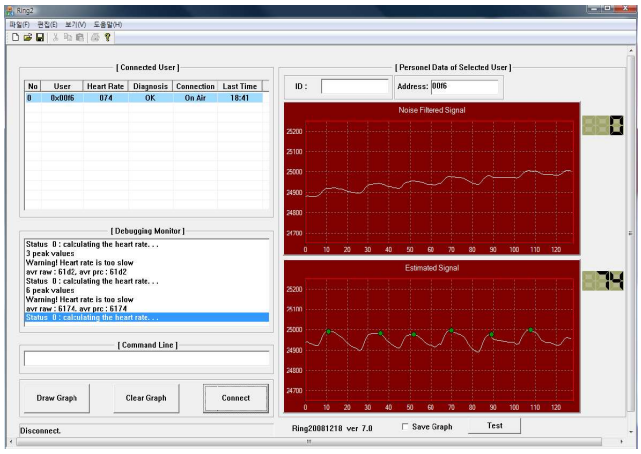

Fig. 7. Monitor program

3) FFT analysis:

Above-mentioned, FFT analysis is one of the most efficient methods for analyzing frequency about periodic signals. Although distortions of signals occur due to the user's movement or environmental changes (particularly variations in the light), the noisy signal continues to possess the heartbeat information. Thus, FFT analysis can be employed to obtain the heart rate. Fig. 8 (a) shows the 256 collected data points at a sampling rate of 25ms and its FFT analysis result. Fig. 8 (b) is drawn up to π, because of its periodic characteristic and its correspondence to the 128 data points, which is half that of the 256 data points.

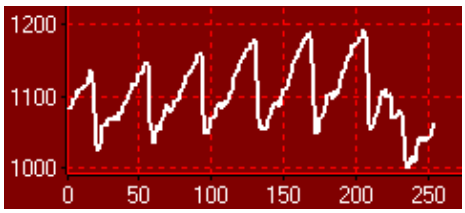

(a) 256 sample data

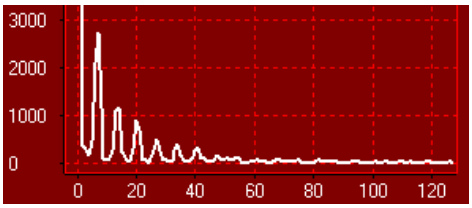

(b) FFT analysis.

Fig. 8. Sampled signal and FFT frequency analysis

If we represent π in terms of frequency, then

$$\pi = \frac{1}{2} \times \frac{1000}{25} [\text{Hz}] \tag{7}$$

For example, in Fig. 8 (b), the biggest peak value is detected at the 7th point except the DC elements; thus, its corresponding frequency becomes (7/128)π. From the (7),

$$\frac{7}{128}\pi = \frac{7}{128} \times \frac{1}{2} \times \frac{1000(m\,\text{sec})}{25} Hz \approx 1.09375 \tag{8}$$

Finally, we can calculate the number of beats per minute by multiplying this value by 60:

$$1.09375 \times 60 = 65.625 \tag{9}$$

Therefore, the number of beats per minute is estimated to be 65.6, which is within the normal range. Thus, the FFT is very useful for estimating the number of beats per minute. However, in this case, certain issues remain. Table 1 shows that at least 2,048 sample data are required to obtain a resolution of approximately 1, and 51.2sec are required. Unfortunately, better resolution requires more power consumption. Our ring sensor receives only 256 samples because the purpose is simply to generate an alert and ask for immediate assistance from the carrier during an emergency state.

Table 1. Resolution according to the number of sampled data

Sampling period (ms)		25			
Number of sample		256	512	1024	2048
Sampling time (ms)		6,400	12,800	25,600	51,200
Sampling Index	1	9.38	4.69	2.34	1.17
	2	18.75	9.38	4.69	2.34
	3	28.13	14.06	7.03	3.52
	4	37.50	18.75	9.38	4.69
	5	46.88	23.44	11.72	5.86
	6	56.25	28.13	14.06	7.03
	7	65.63	32.81	16.41	8.20
	8	75.00	37.50	18.75	9.38
	9	84.38	42.19	21.09	10.55
	10	93.75	46.88	23.44	11.72
	:	:	:	:	:
	20	187.50	93.75	46.88	23.44
	21	196.88	98.44	49.22	24.61
	22	206.25	103.13	51.56	25.78
	:	:	:	:	:
	42	:	196.88	98.44	49.22
	43	:	201.56	100.78	50.39
	:	:	:	:	:
	85	:	:	199.22	99.61
	86	:	:	201.56	100.78
	:	:	:	:	:
	127	:	:	:	148.83
	128				150.00
	:	:	:	:	:
	170				199.22
	171				200.39
	172				201.56
	:	:	:	:	:

4) Signal calibration against motion artifacts:

In particular, the change in the dc level caused by motion artifacts makes it difficult to extract the train of peaks; i.e., the heart beat from sensing data. Jang used a least-squares polynomial of order 3 to solve this problem [12]. From acquired sensing raw data set $\mathbf{y}$, we developed the following expression governing the relationship between time sequences and sensing data at that time:

$$y = c_0 + c_1 x + c_2 x^2 + c_3 x^3 \tag{10}$$

$$\begin{bmatrix} y_1 \\ y_2 \\ \vdots \\ y_{256} \end{bmatrix} = \begin{bmatrix} 1 & 1 & 1^2 & 1^3 \\ 1 & 2 & 2^2 & 2^3 \\ \vdots & \vdots & \vdots & \vdots \\ 1 & 256 & 256^2 & 256^3 \end{bmatrix} \begin{bmatrix} c_0 \\ c_1 \\ c_2 \\ c_3 \end{bmatrix} \tag{11}$$

Eq. (11) can be rewritten as follows:

$$\mathbf{y} = \mathbf{A} \cdot \mathbf{c} \tag{12}$$

Eq. (12) should be modified by incorporating an error vector $\mathbf{e} = \begin{bmatrix} e_0 & e_1 & \cdots & e_{256} \end{bmatrix}^T$ to account for modeling error, as follows:

$$\begin{bmatrix} y_1 \\ y_2 \\ \vdots \\ y_{256} \end{bmatrix} = \begin{bmatrix} 1 & 1 & 1^2 & 1^3 \\ 1 & 2 & 2^2 & 2^3 \\ \vdots & \vdots & \vdots & \vdots \\ 1 & 256 & 256^2 & 256^3 \end{bmatrix} \begin{bmatrix} c_0 \\ c_1 \\ c_2 \\ c_3 \end{bmatrix} + \begin{bmatrix} e_1 \\ e_2 \\ \vdots \\ e_{256} \end{bmatrix} \tag{13}$$

Thus, Eq. (12) can be rewritten as follows:

$$\mathbf{y} = \mathbf{A} \cdot \mathbf{c} + \mathbf{e} \tag{14}$$

The least squares estimator (LSE) $\hat{\mathbf{c}}$ which minimizes $\sum_{i=1}^{256} e_i^2 = \mathbf{e}^T \cdot \mathbf{e} = (\mathbf{y} - \mathbf{A}\mathbf{c})^T (\mathbf{y} - \mathbf{A}\mathbf{c})$ is equal to

$$\hat{\mathbf{c}} = \begin{bmatrix} \hat{c}_1 & \hat{c}_2 & \hat{c}_3 & \hat{c}_4 \end{bmatrix}^T = (\mathbf{A}^T \mathbf{A})^{-1} \mathbf{A}^T \mathbf{y} \tag{15}$$

$(\mathbf{A}^T \mathbf{A})^{-1} \mathbf{A}^T$ is a constant matrix because $\mathbf{A}$ is a constant matrix which is driven from the time index for 256 sensing data. From Eq. (10),

$$\hat{y} = \hat{c}_0 + \hat{c}_1 x + \hat{c}_2 x^2 + \hat{c}_3 x^3 \tag{16}$$

Then, $\hat{\mathbf{y}} = \begin{bmatrix} \hat{y}_0 & \hat{y}_1 & \cdots & \hat{y}_{256} \end{bmatrix}^T$ is calculated at all 256 time step by using Eq. (16). In fact, $\hat{\mathbf{y}}$ is a trend lines representing $\mathbf{y}$.

Now, we can perform data conversion by subtracting the estimated value $\hat{y}$ from the original sensing data y. This data conversion is a process for suppressing motion artifact components from sensing data.

4. Experimental Results

The reflectance type of ring sensor is developed in this study, as shown in Fig. 9. We did not consider the design of the mockup in detail since it was developed to simply

Fig. 9. Ring-type heart rate sensor

(a) Type 1

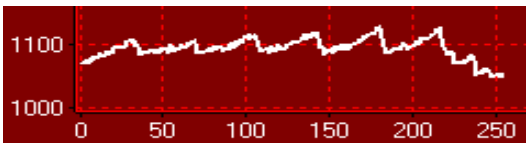

(b) Type 2

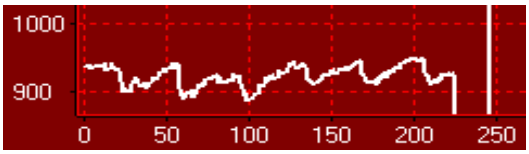

(c) Type 3

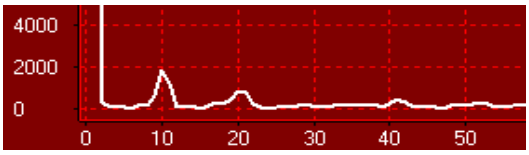

(d) FFT analysis of type 1

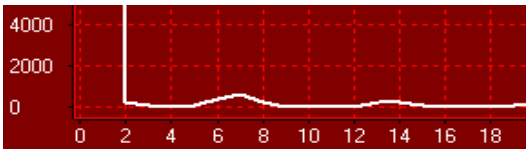

(e) FFT analysis of type 2

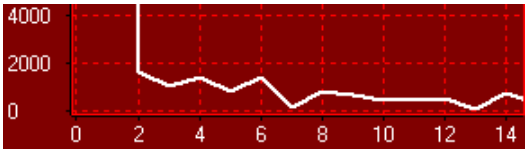

(f) FFT analysis of type 3

Fig. 10. Different types of distorted heartbeat signals and their FFTs

evaluate system performance. Therefore, the shape of the ring is rectangular and it appears to be roughly constructed.

Previous research concentrated on the following problems: the slipping of the ring from the body due to the user's movement, the variation in amplitude depending on the posture of the finger, and the external forces applied to the ring body. In this research, we concentrated on the relationship between the overall movements of the body, including the hand, and signal distortion. In other words, we observed the change in blood volume at the fingertip caused by body movement in real life situations. Moreover, we concentrated our efforts on calculating the number of beats per minute in a highly accurate manner from different types of distorted heartbeat signals.

As the blood rushes to the finger and blood volume is temporarily increased, the total light intensity received at the photodiode decreases and the signal becomes highly distorted. Fig. 10 shows different types of distorted heartbeat signals caused by body movement and the results of their FFT analyses.

From Fig. 10 (a) and (d); the biggest peak value can be detected easily at the 10^{th} point in the case of type 1. However, in Fig. 10 (c) and (f); it is not clear where the biggest peak is. Therefore, FFT analysis does not work in

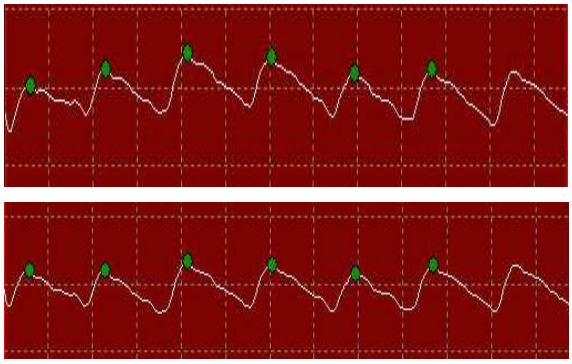

(a) Ideal condition (stop moving)

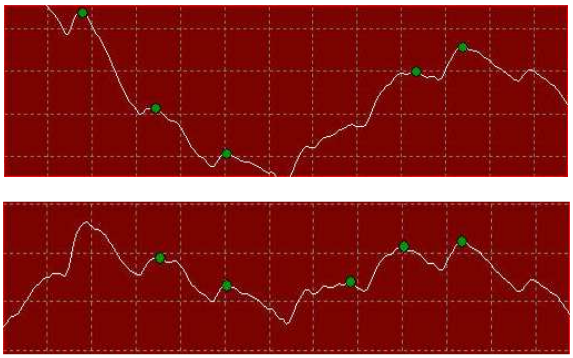

(b) Move hand up and down 1

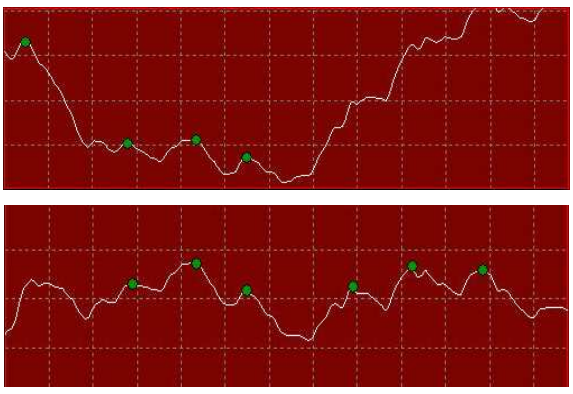

(c) Move hand up and down 2

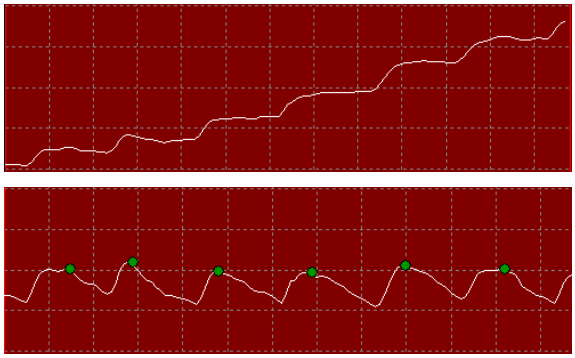

(d) Move hand up and down 3

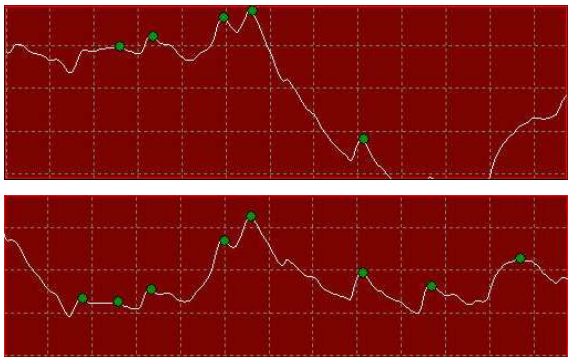

(e) Move hand up and down 4

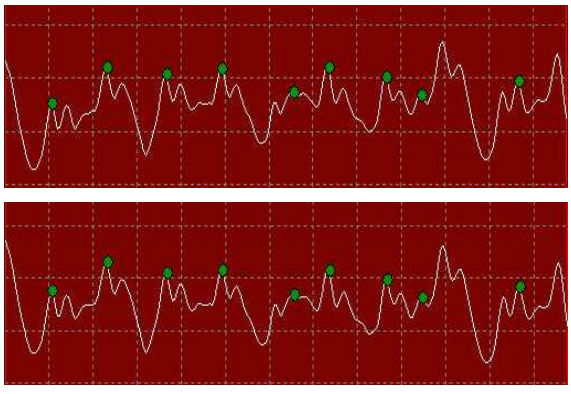

(f) Walk with swinging hand

Fig. 11. Original data and result of data conversion

the case of type 3.

Fig. 11 shows other types of distorted heartbeat signals and the results of their conversion with Eq. (14). Fig. 11 (a) shows clean heartbeat signal without body movement and Fig. 11 (b)~(f) show the distorted heartbeat signals caused by body movement. The green circle is the detectable peak which represents the heartbeat. The upper one part of each figure was captured before data conversion, and the bottom part shows the converted data. The experimental results show that the converted signal with the least squares estimator (LSE) became more stable and was better for detecting peaks.

5. Conclusions

In this paper, the ring-type of PPG heart rate sensor and wireless monitoring system are proposed. We also proposed a robust algorithm to estimate heart rate despite signal distortion caused by movement artifacts, ambient light, slippage of the ring, bending of the finger, etc. Their performance is evaluated and the feasibility of ring sensor is shown through some experimentation. However, we did not accommodate all types of movement, including vigorous exercise. As a result, our experiment shows that the ring sensor is efficient for the chronically ill, and for senior citizens whose movement is relatively minimal.

The proposed system uses the ZigBee-based wireless communication interface, and we expect that the system will be extended to sensor networks for ubiquitous health monitoring. To accomplish this, our ring sensor needs to be more complete and reliable in real dynamic environments. Therefore, we will attempt to improve our system with regard to extracting more reliable heart rates and breath rates [13-15].

Acknowledgements

This research was supported by the Chung-Ang University Scholarship Research Grants in 2012.

References

[1] K. Nakano, T. Murakami, "An Approach to Guidance Motion by Gait-Training Equipment in Semipassive Walking," *IEEE Trans. on Industrial Electronics*, Vol. 55, No. 4, pp. 1707-1714, April 2008.

[2] D. Isern, D. Sánchez, and A. Moreno, "Agents applied in health care: A review," *International Journal of Medical Informatics*, Vol. 79, issue 3, pp. 135-166, March 2010.

[3] C. -M. Chen, "Web-based remote human pulse monitoring system with intelligent data analysis for home health care," *Expert Systems with Applications*, Vol. 38, issue 3, pp. 2011-2019, March 2011.

[4] B. -H. Yang, S. Rhee, and H. Asada, "A Twenty-Four Hour Tele-Nursing System Using a Ring Sensor," *Proc. of 1998 IEEE International Conference on Robotics and Automation*, Leuven, Belgium, May 1998.

[5] S. Rhee, B. -H. Yang, and H. Asada, "Artifact-resistant, power-efficient design of finger-ring plethysmographic sensors. II. Prototyping and benchmarking," *Proc. of the 22nd Annual EMBS International Conference*, Vol. 4, pp. 2796-2799, July 2000.

[6] N. Townsend, "Medical Electronics Lecture Note," 2001, [Online]. Available: http://www.robots.ox.ac.uk/ ~neil/ teaching/lectures/med_elec/lecture5.pdf.

[7] P. A. Oberg. "Blood Flow Measurements," Copyright 2000 CRC Press LLC.

[8] TAOS, Inc., TSL237T light-to-frequency converter Datasheet, [Online]. Available: http://www.taosinc.com

[9] Radiopulse, Inc., MG2455-F48 Datasheet, [Online]. Available: http://www.radiopulse.co.kr.

[10] J. Bachiochi, "Light-to-Frequency Conversion (Part1) TSL230R-Based Pulse Oximeter," *Circuit Cellar, the Magazine for Computer Applications*, pp. 26-31, Dec. 2004.

[11] J. Bachiochi, "Light-to-Frequency Conversion (Part2) TSL230R-Based Pulse Oximeter," *Circuit Cellar, the Magazine for Computer Applications*, pp. 68-71, Jan. 2005.

[12] I. H. Jang, H.G. Yeom and K.B. Sim, "Ring sensor and heart rate monitoring system for sensor network applications," *Electronics Letters*, Vol. 44, No. 24, pp. 1393-1394, November 2008.

[13] W. S. Johnston and Y. Mendelson, "Extracting Breathing Rate Information from a Wearable Reflectance Pulse Oximeter Sensor," *Proc. IEEE 26th Ann Int EMBS Conf*, Sept 2004.

[14] C. Yu, Z. Liu, T. McKenna, A. T. Reisner, and J. Reifman "A method for automatic identification of reliable heart rates calculated from ECG and PPG waveforms," *J. Am. Med. Inform. Assoc.*, Vol. 13, No. 3, pp. 309-320, May-Jun 2006.

[15] S. Bakhtiari, L. Shaolin, T. W. Elmer, N. S. Gopalsami, A. C. Raptis, "A real-time heart rate analysis for a remote millimeter wave I-Q sensor," IEEE Transactions on Biomedical Engineering, Vol. 58, issue 6, pp. 1839-1845, March 2011.

Seung-Min Park He received the B.S. and M.S. degrees from the Department of Electrical and Electronics Engineering, Chung-Ang University, Seoul, Korea, in 2010 and 2012 respectively. He is currently a candidate for the Ph.D. degree in the School of Electrical and Electronics Engineering at Chung-Ang University. His research interests include Pattern Recognition, Brain Computer Interface, etc.

Jun-Yeup Kim He received the B.S. degree from the Department of Electrical and Electronics Engineering, Chung-Ang University, Seoul, Korea, in 2012. He is currently Master course in the School of Electrical and Electronics Engineering at Chung-Ang University. His research interests include Brain-Computer Interface, Particle Swarm Optimization, intelligent System, etc.

Kwang-Eun Ko He received the B.S. and M.S. degrees from the Department of Electrical and Electronics Engineering, Chung-Ang University, Seoul, Korea, in 2007 and 2009 respectively. He is currently a candidate for the Ph.D. degree in the School of Electrical and Electronics Engineering at Chung-Ang University. His research interests include Machine Learning, Emotion Recognition, and Multimodal Intention Recognition, etc.

In-Hun Jang He received the B.S., M. S. and Ph.D. degrees from the Department of Electrical and Electronics Engineering, Chung-Ang University, Seoul, Korea, in 1993, 1999 and 2010 respectively. He is currently a senior researcher in the Korea Institute of Industrial Technology. His research interests include Machine Learning, Multi-agent Robot System and Multimodal Intention Recognition, etc.

Kwee-Bo Sim He received the B.S. and M.S. degrees in Department of Electronic Engineering from Chung-Ang University, Seoul, Korea, in 1984 and 1986 respectively, and Ph. D. degree in Department of Electronic Engineering from the University of Tokyo, Japan, in 1990. Since 1991, he has been a faculty member of the School of Electrical and Electronic Engineering at the Chung-Ang University, where he is currently a Professor. His research interests are Artificial Life, Neuro-Fuzzy and Soft Computing, Evolutionary Computation, Learning and Adaptation Algorithm, Autonomous Decentralized System, Intelligent Control and Robot System, Artificial Immune System, Evolvable Hardware, and Artificial Brain etc.